the fraction of lithium sites increases and the jump distance, λ, between lithium sites decreases. The decrease in jump distance, λ, decreases ΔE_B and E_a (eq 3). The decrease of activation energy with increasing lithium concentration from 5 to 10 mol % $(LiCl)_2$ is due to the decreasing jump distance with increasing lithium content.

At high lithium content (10–20 mol % $(LiCl)_2$), the term $zz_0e^2/(r + r_a)$ in ΔE_B, which describes the Coulombic interaction, increases with increasing lithium content and tends to increase E_a,[29] while the term $zz_0e^2/(\lambda/2)$ also increases with increasing lithium content (i.e. due to the decrease of λ) and tends to decrease E_a. The net result of this competition gives rise to the constant activation energy observed.

Conclusion

The gel-forming region of $(LiCl)_2$–Al_2O_3–SiO_2 xerogels is larger than the corresponding gel-forming region of $(LiCl)_2$–B_2O_3–SiO_2 xerogels. The ionic conductivity of lithium aluminosilicate xerogels is higher with an apparently different mechanism than the corresponding lithium borosilicate xerogels. For samples with constant lithium content (20 mol % $(LiCl)_2$) the ionic conductivity increases with increasing Al_2O_3/SiO_2 ratio due to increasing numbers of mobile lithium ions associated with AlO_4 units or nonbridging oxygens. In contrast, the conductivity in $(LiCl)_2$–B_2O_3–SiO_2 increases with decreasing B_2O_3/SiO_2 ratio due to increasing numbers of mobile lithium ions associated with BO_4 units or nonbridging oxygens.

For xerogels at a fixed Al_2O_3/SiO_2 ratio, the conductivity at 500 °C increases exponentially with the mole fraction of $(LiCl)_2$ and the activation energy decreases rapidly with the increasing $(LiCl)_2$ content from 5 to 10 mol % $(LiCl)_2$. However, E_a remains nearly constant as the $(LiCl)_2$ content increases from 10 to 20 mol %. This constant activation energy is analyzed in terms of the competition between the decreasing jump distance, which tends to decrease the activation energy, and the increasing Coulombic interaction, which tends to increase the activation energy.

Acknowledgment. This work was supported by the National Science Foundation—Materials Chemistry Program DMR 88-08234. We thank Dr. J. Elliot for the FTIR measurements.

Registry No. LiCl, 7447-41-8; Al_2O_3, 1344-28-1; SiO_2, 7631-86-9; ^7Li, 13982-05-3.

Role of Intermediate Phase Formation in the Preparation of $Ba_4Y_2O_7{\cdot}CO_2$†

D. A. Warner and R. E. Riman*

Department of Ceramics, Rutgers, The State University of New Jersey, Piscataway, New Jersey 08855-0909

Received May 24, 1991. Revised Manuscript Received September 3, 1991

The objective of this study was to determine the reaction conditions that facilitate optimal formation of $Ba_4Y_2O_7{\cdot}CO_2$, a compound useful for the preparation of the high-temperature superconductor $YBa_2Cu_3O_{7-x}$. $Ba_4Y_2O_7{\cdot}CO_2$ powders were prepared by conventional, colloid, and coprecipitation powder processing methods to assess the impact of the preparation technique and consequent particle mixing on the $Ba_4Y_2O_7{\cdot}CO_2$ formation mechanism and kinetics. The phase assemblage and phase purity were assessed as a function of solid-state reaction temperature (950–1150 °C) and soak time (2.5–20 h). Phase-pure $Ba_4Y_2O_7{\cdot}CO_2$ was prepared with a 20-h soak at 1050 °C. However, the powder synthesis method played no significant role in phase development. This surprising observation indicates that diffusion of the reactant species probably is not a factor in promoting formation of $Ba_4Y_2O_7{\cdot}CO_2$ as is observed in most solid-state reactions. Instead, $Ba_2Y_2O_5{\cdot}2CO_2$ intermediate phase formation segregates the system to the extent that the degree of homogeneity imparted by all three synthesis methods is equivalent. Formation of the $Ba_2Y_2O_5{\cdot}2CO_2$ intermediate may be related to nucleation and growth kinetics, which can be independent of the powder characteristics or mixedness of the system.

Introduction

Since the discovery of high-temperature superconductivity in the La–Ba–Cu–O system by Bednorz and Müller,[1] a number of oxide superconductors have been discovered.[2-6] The most widely studied oxide has been $YBa_2Cu_3O_{7-x}$, although it does not have the highest transition temperature.

While myriad chemical synthesis routes (e.g., sol–gel, coprecipitation, liquid mix) to prepare $YBa_2Cu_3O_{7-x}$ have been examined in the bulk state,[7-9] conventional powder processing appears able to prepare a material with similar superconducting properties. Thus, for economic reasons, conventional powder processing is the preferred route. However, conventional powder processing is not without drawbacks. A three-component mixture of powders (e.g., $BaCO_3$, CuO, and Y_2O_3) must be reacted at high temper-

† Presented at the 92nd Annual Meeting and Exposition of the American Ceramic Society, April 22–26, 1990, Indianapolis, IN.

(1) Bednorz, J. G.; Müller, K. A. *Z. Phys. B: Condensed Matter* **1986**, *64*, 189.
(2) Wu, M. K.; Ashburn, J. R.; Torng, C. J.; Hor, P. H.; Meng, R. L.; Gao, L.; Huang, Z. J.; Wang, Y. Q.; Chu, C. W. *Phys. Rev. Lett.* **1987**, *58*, 908.
(3) Hor, P. H.; Meng, R. L.; Wang, Y. Q.; Gao, L.; Huang, Z. J.; Bechtold, J.; Forster, K.; Chu, C. W. *Phys. Rev. Lett.* **1987**, *58*, 1891.
(4) Tarascon, J. M.; McKinnon, W. R.; Greene, L. H.; Hull, G. W.; Bagley, B. G.; Vogel, E. M.; Lepage, Y. *Adv. Ceram. Mater.* **1987**, *2* (3B), 498.
(5) Maeda, H.; Tanaka, Y.; Fukutomi, M.; Asano, T. *Jpn. J. Appl. Phys.* **1988**, *27*, L209.
(6) Sheng, Z. Z.; Kiehl, W.; Bennett, J.; El Ali, A.; Marsh, D.; Mooney, G. D.; Arammash, F.; Smith, J.; Viar, D.; Hermann, A. M. *Appl. Phys. Lett.* **1988**, *52*, 1738.
(7) Ritter, J. J. *Ceramic Transactions, Ceramic Powder Science II B*; *Vol. 1*, Messing, G. L., Fuller Jr., E. R., Hausner, H., Eds.; American Ceramic Society: Westerville, OH, 1988; pp 79–84.

0897-4756/92/2804-0197$03.00/0

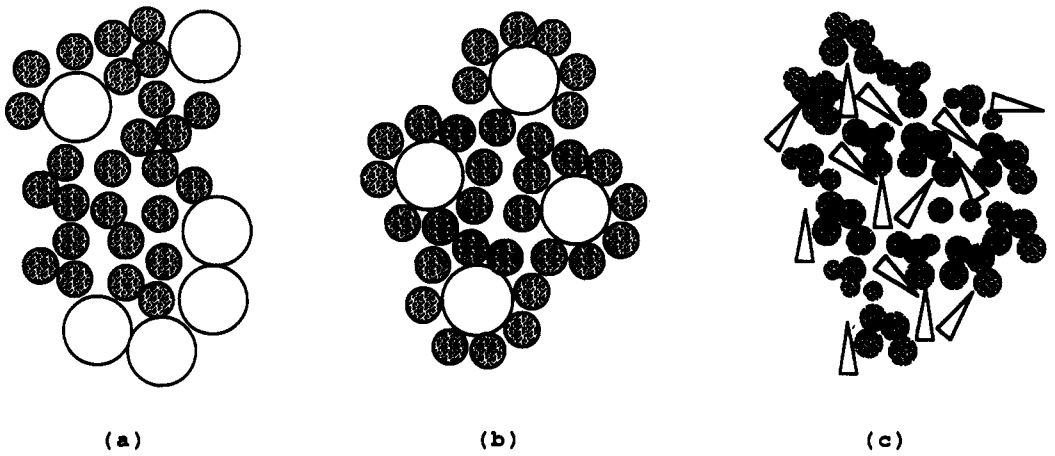

Figure 1. Schematic of mixedness envisioned for mixtures prepared by (a) conventional solid-state synthesis (SSS), (b) selective heterocoagulation (HET), and (c) coprecipitation (COPPT) methods.

ature, milled, and subjected to an additional heat treatment, while chemical methods are capable of preparing single-phase $YBa_2Cu_3O_{7-x}$ in a single solid-state reaction step with significantly high chemical purity. Much of the difficulty with conventional methods can be attributed to barium precursor choice. When carbonates are employed or formed in situ during a solid-state reaction, it is difficult to fully decompose them since their decomposition is kinetically limited.[10]

Another possible hindrance to purity in conventional processing is the greater segregation scale that results from this preparation method. The segregation scale represents the distance over which reactants must diffuse in order to form a multicomponent phase. This scale is determined by the number and size of particles of one composition separating two particles of another composition and increases as the number of components increases. In a conventionally processed mixture, which at best is randomly mixed (Figure 1a), the segregation scale corresponds to a multitude of particle diameters.[11] For two-component mixtures, the segregation scale can be minimized by employing a method known as selective heterocoagulation,[12-14] which results in near ideal mixing (Figure 1b). With selective heterocoagulation, surfactants can be used to control the surface potentials of the two components so that the respective components acquire surface charges of opposite sign. Subsequently, powders flocculate and rapidly settle from suspension.

The use of $Ba_4Y_2O_7{\cdot}CO_2$ as the barium precursor would seem to offer a good compromise between chemical synthesis and conventional powder processing. Due to the 2:1 barium-to-yttrium molar stoichiometry, this compound can be admixed with copper salts or oxides directly, thereby reducing the number of powder components from three to two. $Ba_4Y_2O_7{\cdot}CO_2$ evolves 75 mol % less carbon dioxide per mole of barium than barium carbonate, thus reducing the probability of carbonate stabilization in $YBa_2Cu_3O_{7-x}$ by significant carbon dioxide overpressures.[15] Reports from phase equilibria studies have indicated that the $Ba_4Y_2O_7{\cdot}CO_2$ phase, a line compound incongruently sandwiched between BaO and $Ba_2Y_2O_5{\cdot}2CO_2$, appears to be stable from 920 to 1150 °C when a significant overpressure of CO_2 is present during formation.[16-18] Below 920 °C it decomposes to $Ba_2Y_2O_5{\cdot}2CO_2$ and BaO, while above 1150 °C it forms $Ba_3Y_4O_9$ and BaO. Thus, at room temperature $Ba_4Y_2O_7{\cdot}CO_2$ is metastable, but it decomposes in the presence of moisture.[19] This metastability should provide suitable driving force for optimal $YBa_2Cu_3O_{7-x}$ formation at high temperature.

No prior work has established processing conditions suitable for the formation of the $Ba_4Y_2O_7{\cdot}CO_2$ powder or its use as a precursor for $YBa_2Cu_3O_{7-x}$.[20] The objective of this paper is to investigate various methods to prepare phase-pure $Ba_4Y_2O_7{\cdot}CO_2$, and the reaction mechanisms and kinetics associated with each method when precursor powders are subjected to calcination conditions nominally used in ceramics processing. Evaluation of this material as a precursor for $YBa_2Cu_3O_{7-x}$ will be presented in a future publication.

Experimental Section

$Ba_4Y_2O_7{\cdot}CO_2$ powder was prepared by conventional solid-state synthesis (SSS), selective heterocoagulation (HET), and coprecipitation (COPPT). These methods offered a convenient means to examine the effect of segregation scale (Figure 1) as well as chemistry on the formation of $Ba_4Y_2O_7{\cdot}CO_2$.

(a) Solid-State Synthesis (SSS). Monodisperse $YOHCO_3$ powder was synthesized by the precipitation from homogeneous solution (PFHS) method.[21] An aqueous solution containing 0.03 M Y^{3+} ions and 1.72 M $(NH_2)_2CO$ was prepared by digestion of Y_2O_3 (99.9 wt %, Alfa Products, Danvers, MA) in concentrated HNO_3 (Fisher Scientific, Fairlawn, NJ) followed by dilution with water and addition of an appropriate quantity of $(NH_2)_2CO$ (Aldrich Chemical Co., Milwaukee, WI). This solution was vacuum filtered through a 0.22-μm nylon filter (MSI, Westboro, MA). Subsequently, the solution was heated to 90 °C and aged at this temperature for 1.5 h after precipitation had occurred. The

(8) Behrman, E. C. *Adv. Ceram. Mater.* **1987**, *2* (3B), 539.
(9) Dunn, B.; Chu, C. T.; Zhou, L.-W.; et al. *Adv. Ceram. Mater.* **1987**, *2* (3B), 698.
(10) Kingery, W. D.; Bowen, H. K.; Uhlmann, D. R. *Introduction to Ceramics*; Wiley: New York, 1976.
(11) Hogg, R. *Am. Ceram. Soc. Bull.* **1981**, *60*, 206.
(12) Hogg, R.; Healy, T. W.; Fuerstenau, D. W. *Trans. Faraday Soc.* **1966**, *62*, 1638.
(13) Debely, P. E.; Barringer, E. A.; Bowen, H. K. *J. Am. Ceram. Soc.* **1975**, *68*, C-76-78.
(14) Lange, F. F. *J. Am. Ceram. Soc.* **1989**, *72*, 3.
(15) Hyatt, E. P.; Cutler, I. B.; Wadsworth, M. E. *J. Am. Ceram. Soc.* **1958**, *41*, 70.
(16) Lee, B.-J.; Lee, D. N. *J. Am. Ceram. Soc.* **1989**, *72*, 314.
(17) Roth, R. S.; Davis, K. L.; Dennis, J. R. *Adv. Ceram. Mater.* **1987**, *2* (3B), 303.
(18) Kwestroo, W.; van Hal, H. A. M.; Langereis, C. *Mater. Res. Bull.* **1974**, *9*, 1631.
(19) DeLeeuw, D. M.; Mutsaers, C. A. H. A.; Langereis, C.; et al. *Physica C (Amsterdam)* **1988**, *152*, 39.
(20) Warner, D. A. *The Effects of Intermediate Phase Formation and Particle Mixing on the Synthesis of Dibarium Yttrium Oxycarbonate—A Potential Superconductor Precursor Material*; Rutgers, The State University of New Jersey, New Brunswick, NJ, May 1990.
(21) Sordelet, D.; Akinc, M. *J. Colloid Interface Sci.* **1988**, *122*, 47.

Table I. Characteristics of Precursor Powder Mixtures for $Ba_4Y_2O_7 \cdot CO_2$

		barium salt			yttrium salt		
	mixing	formula	particle size, μm	morphology	formula	particle size, μm	morphology
SSS	nonrandom	$BaCO_3$	1.17[a]	predominantly equiaxed	$YOHCO_3$	0.55	spherical
HET	ordered	$BaCO_3$	1.17[a]	predominantly equiaxed	$YOHCO_3$	0.55	spherical
COPPT	random	$BaCO_3$	~0.3 = c[b] 6 = c/a	rods	YHCN[c]	~0.5[d]	euhedral

[a] Equivalent spherical diameter, mass-weighted average. [b] Estimated from TEM. [c] Yttrium hydroxycarboxynitrate salt, e.g., $Y_2(CO_3)_2(NO_3)(OH)\cdot xH_2O$. [d] Aggregate consisting of 10–25-nm particles.

powder was centrifugally separated, ultrasonically redispersed (Model W-380, Ultrasonics Inc., Farmingdale, NY) and washed twice in doubly distilled deionized (DDD) water and once in acetone (ACS, Fisher Scientific). The resulting powder was dried in air at 90 °C for 24 h. $BaCO_3$ (99.8 wt %) powder was obtained commercially (Fisher Scientific). $BaCO_3$ (15.7872 g) and $YOHCO_3$ (6.6370 g) were mixed using a mortar and pestle for 10 min.

(b) Selective Heterocoagulation (HET). A negatively charged 5 vol % $BaCO_3$ aqueous suspension (19.734 g of $BaCO_3$ (Fisher Scientific), 84.15 mL of DDD H_2O) was prepared by ultrasonically dispersing the powder using 0.95 vol % (0.84 mL) ammonium polyelectrolyte surfactant (Darvan C, R. T. Vanderbilt, M_w = 15000 g/mol, Norwalk, CT). The suspension was aged for approximately 6–12 h, and a pH of 7 maintained with additions of 0.005 M NH_4OH. Subsequently, the powder was ultrasonically redispersed and washed twice in DDD water to remove any residual surfactant. The same procedure was utilized for a pH 7 positively charged 5 vol % $YOHCO_3$ aqueous suspension (8.296 g of $YOHCO_3$ (from the above SSS preparation), 46.24 mL of DDD H_2O) containing 2 vol % (0.99 mL) poly(ethyleneimine) surfactant (PEI, M_w = 50000–60000 g/mol, Eastman Kodak, Rochester, NY). For the separate suspensions of $BaCO_3$ and $YOHCO_3$ particles, the magnitude and polarity of the surfactant-induced surface potentials were inferred from electrosonic amplitude (ESA) measurements (Model ESA-8000, Matec, Framingham, MA). These measurements indicated that, after redispersal, the washed powders maintained their respective sign of mobility charge and magnitude for periods exceeding 6 h. Visual inspection of the suspension turbidity revealed that colloidal stabilities remained after 24 h. To initiate heterocoagulation, 89.44 mL of the $BaCO_3$ was added to 49.36 mL of a gently stirred $YOHCO_3$ suspension. The system was fully flocculated in about 10 s, with a resultant floc size of ~450 μm as estimated by optical microscopy and sedimentation rate. The flocculated composite powder was vacuum filtered with a 0.22-μm nylon membrane and dried in air at 90 °C for 24 h.

(c) Coprecipitation (COPPT). A reverse strike coprecipitation was performed by addition of a "metal cation" solution containing Y^{3+} and Ba^{2+} ions to an "anion" solution containing CO_3^{2-} and OH^- ions. The metal cation solution was formed by dissolving a 2:1 molar ratio of $Ba(NO_3)_2$ (Fisher Scientific) and $Y(NO_3)_3{\cdot}6H_2O$ (99.9 wt %, Alfa Products, Danvers, MA) in DDD water. The total cation concentration was 0.1 M (e.g., 3.33×10^{-2} M Y^{3+}, 6.66×10^{-2} M Ba^{2+}). The cation solution was adjusted to pH 5 using sparing amounts of 0.05 M HNO_3. To ensure quantitative precipitation of the cations, the carbonate concentration in the anion solution was maintained at a level twice that required to precipitate all of the barium ions as barium carbonate. Thus a 0.133 M CO_3^{2-} anion solution was prepared by the addition of 2.791 g of NH_4HCO_3 (Fisher Scientific) to 250 mL of DDD H_2O. To avoid silicon contamination problems normally encountered with glassware, 1000-mL poly(methylpentene) bottles (Fisher Scientific) were used.

The coprecipitation was initiated by rapid addition of 250 mL of cation solution to an equal amount of anion solution vigorously stirred by magnetic means at room temperature. The suspension was adjusted to pH 10 with 15 mL of reagent grade concentrated NH_4OH to ensure a maximum concentration of CO_3^{2-} species for complete precipitation of all metal cation species from solution. The precipitate was aged at room temperature with stirring for 2 h. The powder was centrifugally separated, washed, and ultrasonically redispersed and dried in air at 90 °C for 24 h.

(d) Solid-State Reaction of the Precursor Powders. To allow for comparison among methods, all solid-state reaction studies were conducted using single powder batches prepared by each of the three methods described above. Solid-state reactions were performed in 99 wt % pure alumina boats (Berkeley Advanced Ceramics, Berkeley, CA) under static air in a sealed tube furnace (Rapid Temp Model 1700, CM Furnaces Inc., Bloomfield, NJ) calibrated to ±2.5 °C over the temperature range 950–1150 °C with a K-type thermocouple and Model 51 analyzer (Fluke Co., Everett, WA). To study the phase progression exhibited by each mixture, precursor powders were calcined under conditions approaching those nominally employed in ceramics processing using a heating rate of 20 °C/min and maintaining a desired temperature for a soak time of 20 h. The soak temperature was varied in 50 °C intervals over the temperature range 950–1150 °C. The three precursor powders, SSS, HET, and COPPT, were fired simultaneously in the same heating zone for a given temperature to ensure identical reaction conditions. The carbon dioxide partial pressure necessary to stabilize the $Ba_4Y_2O_7{\cdot}CO_2$ phase was provided by the decomposition of the carbonate precursors, since carbon dioxide is a relatively dense gas and lingers in the powder periphery. The calcined powders were cooled rapidly in ambient air and stored in a vacuum desiccator to avoid hydroscopic degradation.[19] Calcined powders were characterized immediately thereafter. The reaction mechanism was studied by subjecting the SSS powder to a 20 °C/min heating rate to a temperature of 1050 °C for soak times of 2.5, 5, 10, and 20 h.

(e) Powder Characterization. Mass-weighted mean particle sizes were determined with X-ray photosedimentation (Sedigraph 5100, Micromeritics, Inc., Norcross, GA). Microporosity was determined with single-point nitrogen adsorption measurements using the BET method (Quantasorb Surface Area Analyzer, Quantachrome Inc., Syosset, NY). Measurements were conducted with a 0.3 volume fraction N_2/He gas mixture. Samples were outgassed in helium. Morphology was assessed with scanning electron microscopy (SEM, Model 1200, Amray, Bedford, MA) and transmission electron microscopy (TEM, Model EM-002B, Akashi Beam Technology Corp., Tokyo, Japan). The TEM was also equipped with energy-dispersive X-ray spectroscopy (EDS) capability for detection of cation species (PGT Inc., Princeton, NJ). Carbon, hydrogen, and nitrogen content were determined using combustion analysis (Oneida Research Services, Whitesboro, NY). The formula weights of reagents and the concentrations of volatile species in product powders were measured by thermal gravimetric analysis using a heating rate of 20 °C/min and a final temperature no greater than 1150 °C (Perkin Elmer TGA-7, Norwalk, CT; Netzsch Model STA-409, Exton, PA). Phase assemblages were determined with X-ray diffraction (XRD, Model D-500, Siemens, AG, Karlsruhe, FRG) using Ni-filtered Cu Kα radiation and operated at 40 kV, 30 mA. The data were collected by means of a DACO microprocessor using a stepwidth of 0.05 2θ/step and a measuring time of 1 s/step. Joint Committee Powder Diffraction Standards (JCPDS) powder diffraction files were consulted for all phase analyses. However, two unindexed diffraction peaks were observed on XRD patterns for phase-pure $Ba_4Y_2O_7{\cdot}CO_2$ that corresponded to d spacings of 6.971 and 3.299 Å with approximate relative intensities of 12 and 1%, respectively.

Results and Discussion

Characteristics of Precursor Powders. The characterization data in Table I show that the three synthetic methods employed provide appropriate systems for examining the effect of segregation scale on the preparation of $Ba_4Y_2O_7{\cdot}CO_2$. Comparison of the SSS and HET systems allows study of the effect of mixing method, while com-

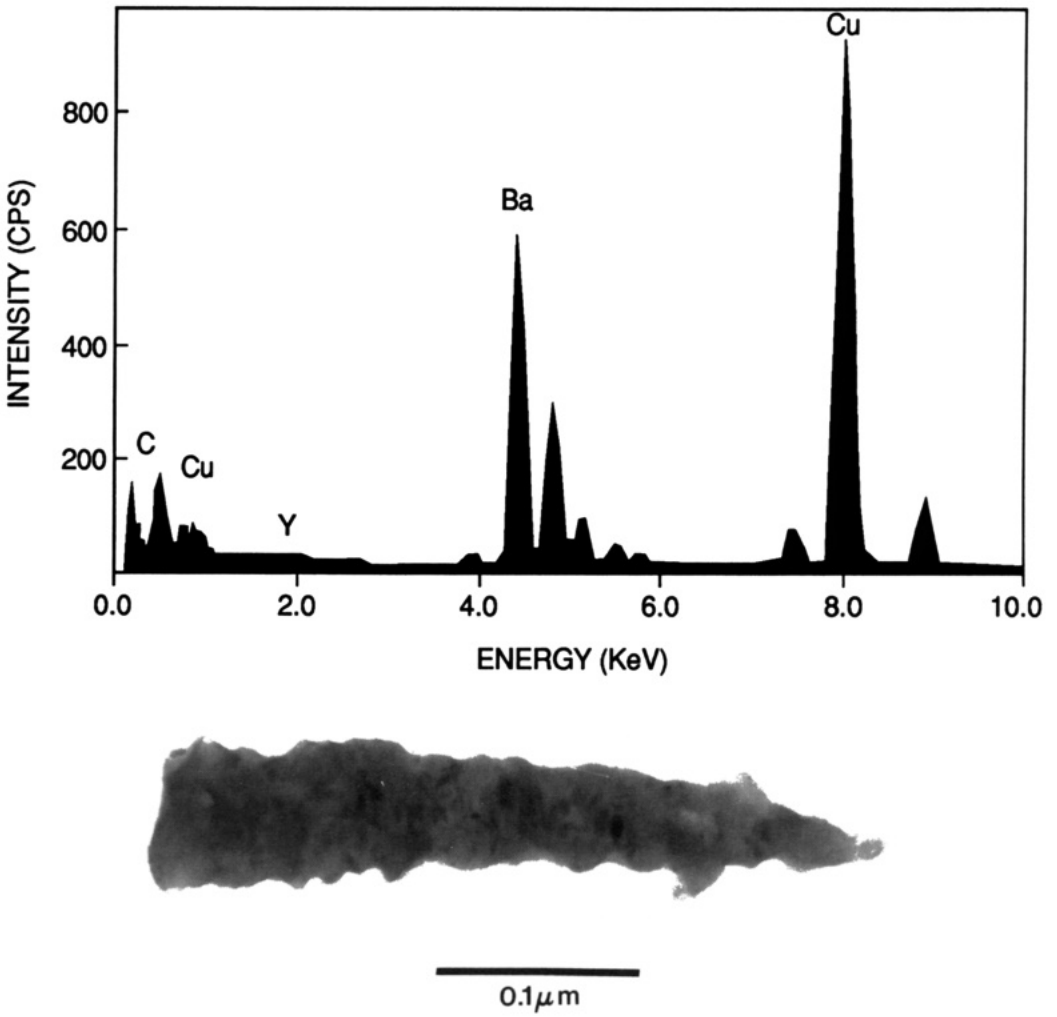

Figure 2. TEM photomicrograph of a typical rodlike particle found in COPPT powder. EDS spectrum of particle is characteristic of barium component. Copper peaks are due to sample grid.

parison of SSS/HET systems to COPPT allows study of the effects of mixing method, initial particle size, and initial particle morphology. Both the SSS and HET methods utilized 1.17-μm equiaxed barium carbonate and 0.55-μm yttrium hydroxycarbonate. The surface areas for SSS and HET systems were 3.01 and 2.88 m^2/g, respectively. The surface area calculated from the mean particle sizes was $\sim$1.6 m^2/g for both powders. Therefore, although some particle microporosity existed in these mixtures, the major difference lies in the manner in which these components were mixed (Figure 1). The segregation scale for the SSS method was expected to be magnitudes larger than for the HET method.

Results of the COPPT method deserve greater elaboration, since the initial particle size and morphology differed from those found for SSS and HET methods, with minor differences in the chemical composition as well. X-ray diffraction of the powder revealed only one crystalline phase, namely, barium carbonate. TEM/EDS/SAED measurements revealed that the powder was diphasic in nature. Particles that exhibited rodlike morphologies were found to contain only barium cations (Figure 2). These particles had an average length of 0.3 μm and an aspect ratio (c/a) of $\sim$6. SAED patterns consisting of discontinuous rings were characteristic of polycrystalline materials. However, these rings were unindexable for a phase determination. On the basis of the XRD data and literature indicating the tendency of barium carbonate to precipitate as rodlike morphologies,[22] it was concluded that the rodlike particles in the COPPT powder were barium carbonate. The second phase, $\sim$0.5-μm euhedral aggregates containing 10–50-nm primary particles (Figure 3), was found to consist of yttrium cations and a small amount of barium cations (<5 wt %, accounting for barium fluorescence). On the basis of the fine ultrastructure of the aggregates, the presence of the barium component was attributed to occlusion within the 10–50-nm primary particles. This phase exhibited a diffuse SAED pattern and no XRD pattern, indicating that the salt was amorphous. Thermal gravimetric analysis traces of the coprecipitated powder exhibited multistage decomposition behavior, with most of the weight loss occurring below 600 °C. This behavior was characteristic of yttrium hydroxycarbonate salts prepared in this study and reported in more detail by Sordelet and Akinc.[21] Combustion analysis of coprecipitated powders prepared under various conditions not cited in this paper indicate that this powder is a hydroxycarboxynitrate salt (e.g., $Y_2(CO_3)_2NO_3OH\cdot xH_2O$) of a highly variable composition. Yttrium in the presence of carbonate and nitrate ions is known to precipitate as a salt containing these anions.[23,24]

(22) Conaway, W. A.; Johnson, A. J.; Smisko, J. Process of Preparing $BaCO_3$ by Carbonation of Aqueous BaS. U.S. Patent No. 3,421,843, Jan 14, 1969.
(23) Chou, K. S.; Burkhardt, L. E. *Thermochim. Acta* **1982**, *55*, 75.

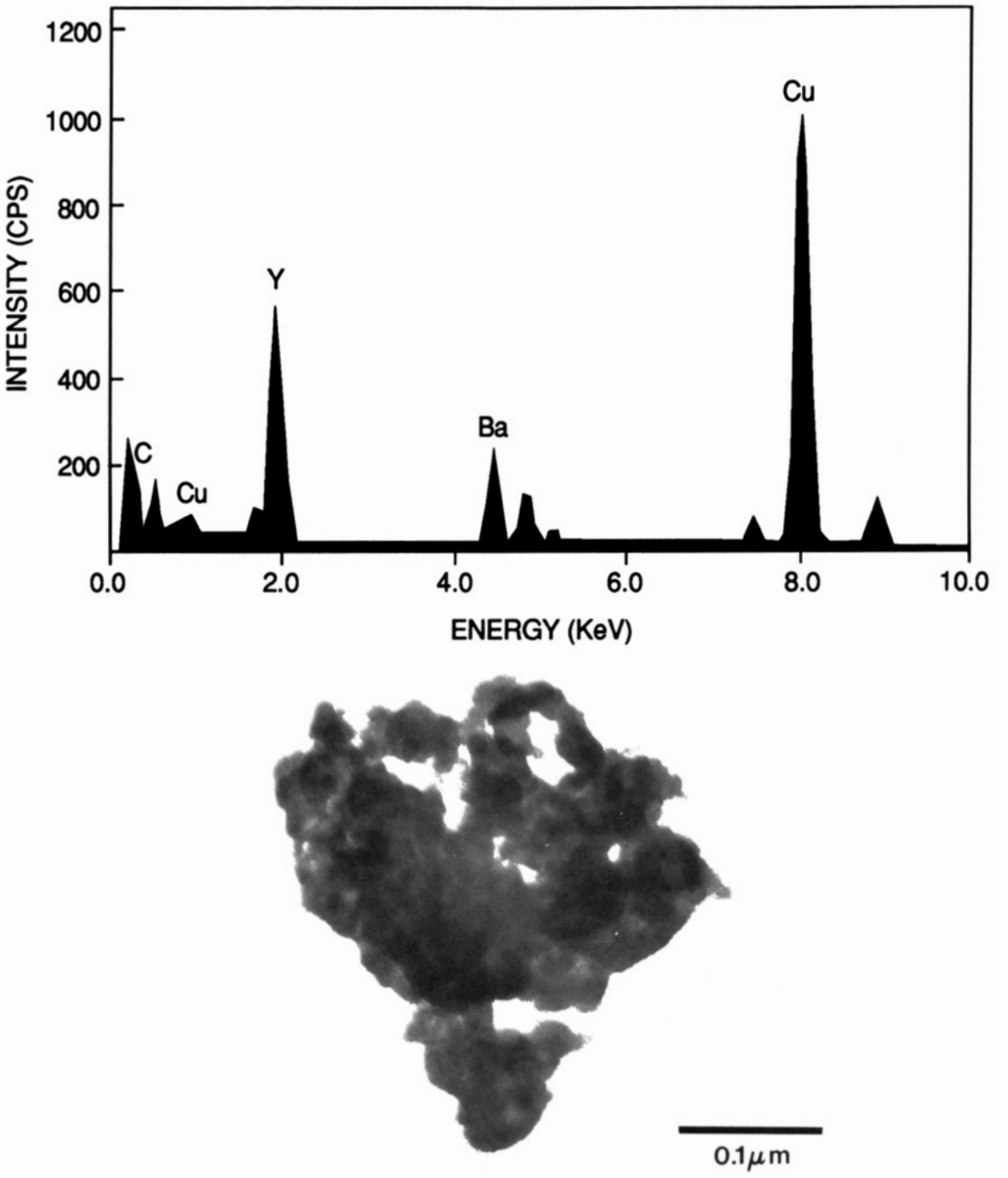

Figure 3. TEM photomicrograph of typical euhedral aggregate found in COPPT powder. EDS spectrum of particles is characteristic of yttrium with small concentrations of barium ions present. Copper peaks are due to sample grid.

SEM characterization of the COPPT powder qualitatively indicated that the particle mixing was homogeneous in a random nature. In addition, the powder had a surface area of 59.2 m^2/g, which was ~20 times greater than the SSS or HET mixtures. The nature of the coprecipitation process and the low probability of submicron powders to segregate leads one to speculate that this mixture was random.

Solid-State Reactivity of Precursor Powders. (a) Observed Phase Transformations. The reactivity and resultant phase composition of the three precursor powders were similar, despite the significant differences in segregation scale and chemistry (Table II). XRD patterns of the COPPT samples, indicative of all the precursor powders over the temperature range 950–1150 °C, are shown in Figure 4. At temperatures greater than 750 °C but less than 950 °C, all systems consisted of a mixture of barium carbonate and yttrium oxide. Thus the hydroxide, carbonate, and nitrate groups associated with the yttrium salt had decomposed. At 950 °C, $Ba_2Y_2O_5{\cdot}2CO_2$ was the primary phase coexisting with $BaCO_3$ and Y_2O_3. When a temperature of 1050 °C was reached, all Y_2O_3 was consumed and only $Ba_2Y_2O_5{\cdot}2CO_2$ and $BaCO_3$ were present. At 1050 °C, single-phase $Ba_4Y_2O_7{\cdot}CO_2$ was prepared, although traces of barium peroxide were observed in HET and SSS samples. All three processing methods yielded highly aggregated powders with similar morphologies but differing slightly in crystallite size (Figure 5). Nondescript particles were intermixed with rectangular prismatic particles similar to the tetragonal $Ba_4Y_2O_7{\cdot}CO_2$ unit cell. BET surface areas for SSS, HET, and COPPT methods

(24) Dragoo, A. L.; Domingues, C. P. *J. Am. Ceram. Soc.* **1982**, *65*, 253.

Table II. Phase Composition of Precursor Powders at Various Calcination Temperatures

reaction temp/method	major phase[a]	minor phase[a]	trace phase[a]
T = 950 °C			
solid-state synthesis	B2Y2, BC, YO		
heterocoagulation	B2Y2, BC, YO		
coprecipitation	B2Y2, BC, YO		
T = 1000 °C			
solid-state synthesis	B2Y2	BC	
heterocoagulation	B2Y2, BC		
coprecipitation	B2Y2, BC		
T = 1050 °C			
solid-state synthesis	B4Y2		BP
heterocoagulation	B4Y2		BP
coprecipitation	B4Y2		
T = 1100 °C			
solid-state synthesis	B4Y2		BP
heterocoagulation	B4Y2		BP
coprecipitation	B4Y2	B3Y4, BP	
T = 1150 °C			
solid-state synthesis	B4Y2	B3Y4, BP	
heterocoagulation	B4Y2	B3Y4, BP	
coprecipitation	B3Y4, BP	BO	B4Y2

[a] Key: YO = Y_2O_3; BC = $BaCO_3$; BP = BaO_2; BO = BaO; B2Y2 = $Ba_2Y_2O_5{\cdot}2CO_2$; B3Y4 = $Ba_3Y_4O_9$; B4Y2 = $Ba_4Y_2O_7{\cdot}CO_2$.

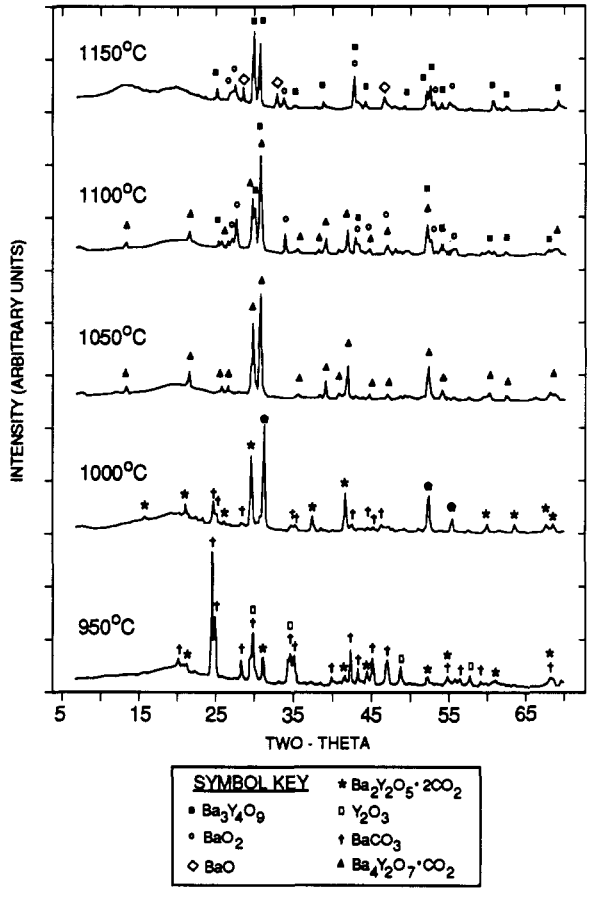

Figure 4. XRD overlay of COPPT powder mixture heated at 20 °C/min and soaked for 20 h at various reaction temperatures.

were 0.7, 0.7, and 1.3 m^2/g. Using a density of 5.109 g/cm^3,[25] crystallite sizes of 1.7, 1.7, and 0.88 μm were computed for the respective methods. The smaller particle size obtained for COPPT may be attributed to the finer particle size of the initial mixture.

At temperatures of 1100–1150 °C, decomposition of $Ba_4Y_2O_7{\cdot}CO_2$ was observed. This was especially noticeable in the COPPT powder, where $Ba_4Y_2O_7{\cdot}CO_2$ substantially decomposed to $Ba_3Y_4O_9$, BaO, and BaO_2 with the 50 °C increase in temperature. The smaller particle size for COPPT may account for the more substantial decomposition of $Ba_4Y_2O_7{\cdot}CO_2$ when heated above 1050 °C relative to the HET and SSS methods.

Table III. Phase Composition of Precursor Powders Calcined at 1050 °C for Various Times

reaction time, h	major phase[a]	minor phase[a]
0	BC, YHC	
2.5	B2Y2, BC, YO	
5	B2Y2, BC, YO	
10	B2Y2, B4Y2	BC
20	B4Y2	

[a] Key: YO = Y_2O_3; BC = $BaCO_3$; B2Y2 = $Ba_2Y_2O_5{\cdot}2CO_2$; B4Y2 = $Ba_4Y_2O_7{\cdot}CO_2$; YHC = $YOHCO_3$.

The presence of BaO_2 was considered to be an artifact of $Ba_4Y_2O_7{\cdot}CO_2$ decomposition, since the concentration of $Ba_4Y_2O_7{\cdot}CO_2$ decreased as the concentrations of $Ba_3Y_4O_9$ and BaO_2 increased. Barium peroxide is not observed at these temperatures, since thermodynamic computations reveal that it is unstable in air above ~640 °C,[26] and it has been observed to decompose at temperatures from 735 to 800 °C.[27,28] It is possible that the highly active BaO produced from $Ba_4Y_2O_7{\cdot}CO_2$ decomposition reacted with ambient oxygen during rapid cooling in ambient air to produce barium peroxide. The highly active nature of the barium oxide phase has been observed previously.[29] Thermal gravimetric analysis substantiated not only the oxidation of BaO during cooling but also the thermodynamic reversibility of the process. A COPPT sample was heated in static air for 10 h to form a mixture of $Ba_3Y_4O_9$ and what was believed to be BaO. This mixture exhibited a 2.87 wt % weight gain upon rapid cooling in ambient air, which indicated a reaction with the atmosphere. This is close to the expected theoretical weight gain of 3.30 wt %, assuming complete BaO oxidation to BaO_2. Upon heating at 20 °C/min, this mixture exhibited a 3.70 wt % weight loss at a temperature of 675 °C.

(25) Kovba, L. M.; Lykova, C. N.; Antipov, E. V. *Zh. Neorg. Khim.* **1983**, *28*, 724.

(26) Fine, A. F.; Geiger, G. H. *Handbook on Material and Energy Balance Calculations in Metallurgical Processes*; The Metallurgical Society of AIME: Warrendale, PA, 1979; p 391.

(27) Weast, R. C., Ed. *Handbook of Chemistry and Physics*; CRC Press: Boca Raton, FL, 1985; p *B-75*.

(28) Roth, R. S.; Rawn, C. J.; Hill, M. D. *Chemistry of Electronic Ceramic Materials*; Davies, P. K., Roth, R. S., Eds.; NIST SP 804, Jan 1991; U.S. Printing Office: Washington, D.C., 1991; pp 225–236.

(29) Garn, P. D.; Habash, T. S. *J. Phys. Chem.* **1979**, *83*, 229.

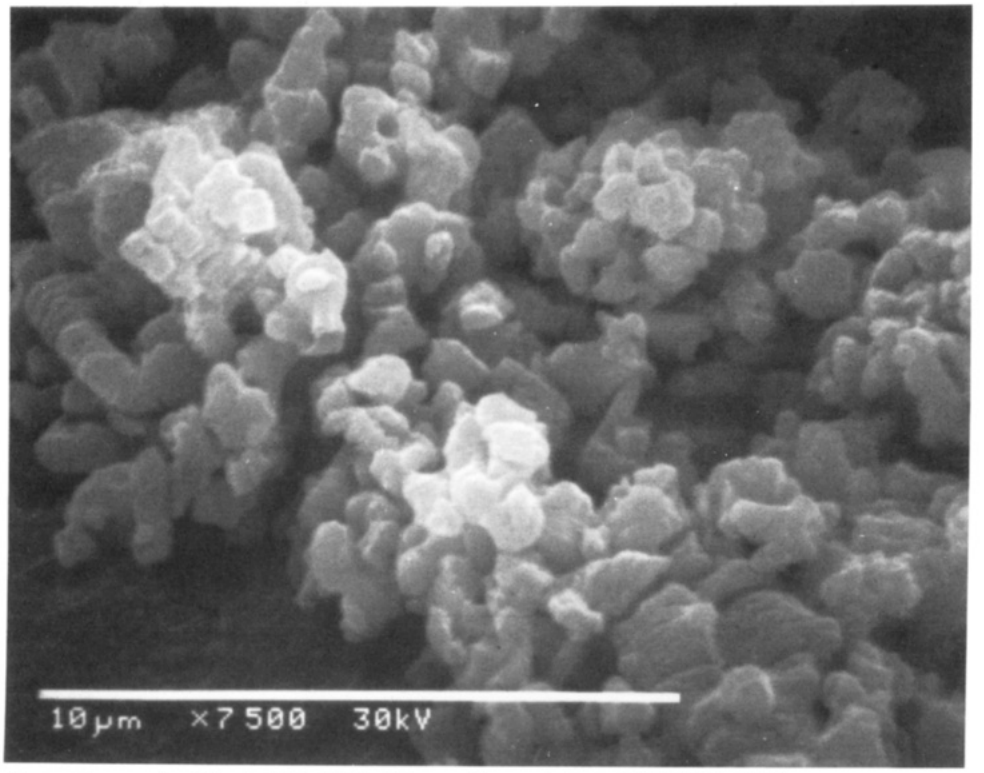

Figure 5. SEM photomicrograph of typical $Ba_4Y_2O_7{\cdot}CO_2$ powder soaked at 1050 °C for 20 h.

On the basis of the above data, it was concluded that the optimum reaction temperature for $Ba_4Y_2O_7{\cdot}CO_2$ formation was 1050 °C. This falls within the temperature range in the earlier cited literature.[16-18] However, the stability range determined in this study was considerably narrower (<±50 °C).

(b) Reaction Mechanism. Given an optimum reaction temperature of 1050 °C, work was focused on determining the appropriate reaction time for $Ba_4Y_2O_7{\cdot}CO_2$ synthesis and gaining better insight into the reaction mechanism. As the carbonates in the SSS powder decomposed, the first multicomponent phase, $Ba_2Y_2O_5{\cdot}2CO_2$, was not observed in substantial amounts until after a 5-h soak time (Table III and Figure 6). Initial $Ba_4Y_2O_7{\cdot}CO_2$ formation was observed after a 10-h reaction time and was completed in 20 h. As with the soak temperature studies mentioned above, yttrium oxide was not found to coexist with $Ba_4Y_2O_7{\cdot}CO_2$, indicating that $Ba_2Y_2O_5{\cdot}2CO_2$ was the sole source of yttrium for $Ba_4Y_2O_7{\cdot}CO_2$ formation. Thus, the formation of $Ba_4Y_2O_7{\cdot}CO_2$ appeared to be rate-limited by the formation and decomposition of $Ba_2Y_2O_5{\cdot}2CO_2$.

The 20 °C/min heating rate employed may have provided an opportunity for $Ba_2Y_2O_5{\cdot}2CO_2$ to form, since its thermodynamic stability range is encountered prior to that of $Ba_4Y_2O_7{\cdot}CO_2$. However, on the basis of our experimental observations and phase boundaries evident in the calculated $BaO{-}Y_2O_3$ phase diagram,[16] the region of $Ba_2Y_2O_5{\cdot}2CO_2$ stability at best is from 750 to 920 °C (ΔT = 170 °C). Thus, at a heating rate of 20 °C/min, thermodynamic stability conditions promoting $Ba_2Y_2O_5{\cdot}2CO_2$ formation should exist during a period of 8.5 min, a duration over which this system reacts to small extent. Since $Ba_2Y_2O_5{\cdot}2CO_2$ formed in a temperature range in which it is thermodynamically unstable (950–1050 °C), the experimental results suggest that it is kinetics rather than thermodynamics that limit the process.

On the basis of data from the three synthesis methods examined, the following chemistry is relevant to the formation of $Ba_4Y_2O_7{\cdot}CO_2$ from mixtures of $BaCO_3$ and Y_2O_3

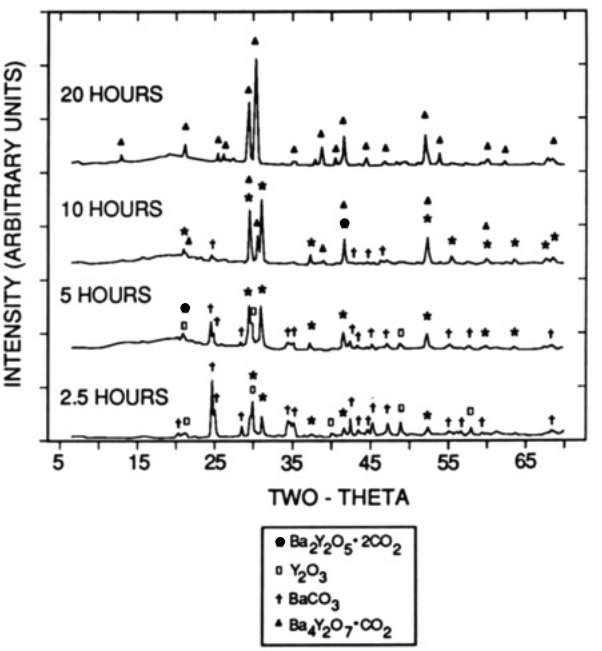

Figure 6. XRD overlay of SSS powder mixture heated at 20 °C/min and soaked at 1050 °C for various reaction times.

above 750 °C with an overpressure of carbon dioxide from the yttrium salt:

T < 1050 °C

$$4BaCO_3 + Y_2O_3 = Ba_2Y_2O_5{\cdot}2CO_2 + 2BaCO_3 \quad (1)$$

1000 °C < T < 1100 °C

$$2BaCO_3 + Ba_2Y_2O_5{\cdot}2CO_2 = Ba_4Y_2O_7{\cdot}CO_2 + 3CO_2 \quad (2)$$

T > 1100 °C

$$2Ba_4Y_2O_7{\cdot}CO_2 = Ba_3Y_4O_9 + 5BaO + 2CO_2 \quad (3)$$

The lack of a role played by the powder synthesis method in the reaction kinetics was a surprising result. It is

usually anticipated that chemical synthesis methods such as COPPT will produce a material exhibiting better phase and chemical purity than materials produced with more conventional methods such as SSS or HET. In this case, however, formation and decomposition of $Ba_2Y_2O_5{\cdot}2CO_2$ kinetically limited the formation of $Ba_4Y_2O_7{\cdot}CO_2$. Thus, intermediate $Ba_2Y_2O_5{\cdot}2CO_2$ formation served to segregate the powder mixtures regardless of the mixing structure existing as a result of the processing method. Intermediate compound formation of this type has been observed in the preparation of Ba_2SiO_4 from $BaCO_3$–SiO_2 mixtures,[30] in which $BaSiO_3$ was the intermediate compound found to coexist with $BaCO_3$. In that case, Ba_2SiO_4 began to form only after complete consumption of the SiO_2. Similar solid-state chemistry has been observed in the synthesis of β-wollastonite.[31]

In the preparation of $Ba_4Y_2O_7{\cdot}CO_2$, formation of the intermediate phase $Ba_2Y_2O_5{\cdot}2CO_2$ was also independent of the synthesis method. This indicates that the reaction kinetics of $Ba_2Y_2O_5{\cdot}2CO_2$ was not controlled by the diffusion rate of reactant species but instead by factors that influence the nucleation and/or growth of the $Ba_2Y_2O_5{\cdot}2CO_2$ phase. For instance, nucleation site density for $Ba_2Y_2O_5{\cdot}2CO_2$ could strongly influence the nucleation rate, and this parameter can be independent of the characteristics of the powder. Rate-limiting product nucleation has been observed in solid-state reactions between $BaCO_3$ and ZnO.[32]

Conclusions

Solid-state reaction of individual powders prepared by SSS, HET, and COPPT methods produced a $Ba_4Y_2O_7{\cdot}CO_2$ powder with similar characteristics. The optimal reaction conditions for formation of $Ba_4Y_2O_7{\cdot}CO_2$ were a 20-h soak at 1050 °C. The reaction conditions were found to be independent of the preparation method, due to the formation of the $Ba_2Y_2O_5{\cdot}2CO_2$ intermediate phase in all systems. Formation of $Ba_2Y_2O_5{\cdot}2CO_2$ was also independent of the synthesis method and was controlled instead by factors such as nucleation site density, which can be independent of the powder characteristics or mixedness.

Acknowledgment. We acknowledge the generous support of Engelhard Corp., the New Jersey State Commission on Science and Technology, and the Center for Ceramic Research. The assistance of Ms. K. Griffin in the preparation of the manuscript is gratefully appreciated.

Registry No. Y_2O_3, 1314-36-9; $(NH_2)CO$, 57-13-6; $YOHCO_3$, 136632-09-2; $Ba(CO_3)$, 513-77-9; $Ba(NO_3)_2$, 10022-31-8; $Y(NO_3)_3$, 10361-93-0; NH_4HCO_3, 1066-33-7; $Y_2(CO_3)_2NO_3OH$, 136826-97-6; $Ba_4Y_2O_7{\cdot}CO_2$, 117128-24-2; $Ba_3Y_4O_9$, 11071-75-3; BaO, 1304-28-5; $Ba_2Y_2O_5{\cdot}2CO_2$, 117128-25-3; BaO_2, 1304-29-6.

(30) Yamaguchi, T.; Fujii, H.; Kuno, H. *J. Inorg. Nucl. Chem.* **1972**, *34*, 2739.
(31) Ibanez, A.; Gonzalez Pena, J. M.; Sandoval, F. *Am. Ceram. Soc. Bull.* **1990**, *69*, 374.
(32) Hulbert, S. F.; Klawitter, J. J. *J. Am. Ceram. Soc.* **1967**, *50*, 484.

Ordered Bimetallic–Radical Species Forming Low-Dimensional Magnetic Materials

Andrea Caneschi,† Dante Gatteschi,*,† Paul Rey,‡ and Roberta Sessoli†

Department of Chemistry, University of Florence, via Maragliano 75, Florence, Italy, and Centre d'Etudes Nucleaires, Grenoble, France

Received June 11, 1991. Revised Manuscript Received October 24, 1991

2-(4-Pyridyl)-4,4,5,5-tetramethylimidazoline-1-oxyl 3-oxide, NITpPy, reacts with metal hexafluoroacetylacetonates, $M(hfac)_2$, forming compounds of formula $Mn_2M(hfac)_6(NITpPy)_2$, with M = Mn, Co, Ni. No crystals suitable for X-ray analysis could be obtained, but powder diffraction data suggested that all the compounds are isomorphous. On the basis of magnetic and IR evidence, we assume that in all these compounds $Mn(hfac)_2(NITpPy)$ chains are present in which the radicals bridge two manganese(II) ions through the NO groups. The pyridine nitrogen donors bind the M atoms to connect different chains. In this way either ladders or two-dimensional structures can be formed. All the compounds order magnetically below 10 K, giving rise to spontaneous magnetization.

Introduction

Magnetic molecular materials have been the object of increasing interest in the last few years. In fact these systems can potentially associate bulk ferro- or ferrimagnetism or weak ferromagnetism with chemical and optical properties typical of molecular compounds and eventually they can be exploited in devices. Currently several different synthetic approaches are followed in order to synthesize this type of material,[1] which can be classified as organic,[2] organic–organometallic,[3] organic–inorganic,[4]

† University of Florence.
‡ Centre d'Etudes Nucleaires.

(1) *Magnetic Molecular Materials*; Gatteschi, D., Kahn, O., Miller, J. S., Palacio, F., Eds.; Kluwer: Dordrecth, The Netherlands, 1991.
(2) Sugawara, T.; Bandow, S.; Kimura, K.; Iwamura, H.; Itoh, K. *J. Am. Chem. Soc.* **1986**, *108*, 368. Dougherty, D. A. *Mol. Cryst. Liq. Cryst.* **1989**, *176*, 25. Veciana, J.; Rovira, C.; Armet, O.; Domingo, V. M.; Crespo, M. I.; Palacio, F. *Mol. Cryst. Liq. Cryst.* **1989**, *176*, 77. Le Page, T. J.; Breslow, R. *J. Am. Chem. Soc.* **1987**, *109*, 6412. Torrance, J. B.; Bagus, P. S.; Johannsen, I.; Nazzal, A. I.; Parkin, S. S. P. *J. Appl. Phys.* **1988**, *63*, 2962.

0897-4756/92/2804-0204$03.00/0